MEDP6450 Computational Methods in Medical Physics
Justin Tam B00782164
Feb 4 2026

Lab 2 – Model-Based Does Calculation

Code Introduction

1. The code is organized as a single class (`DoseMap`) representing the patient details and geometry, including the 2D dose maps to be calculated.

2. The core equations given in this report are referenced to a specific line, which refers to a specific line in the code of the only python file, main.py.

Deliverable 1: Display of DPB Kernels

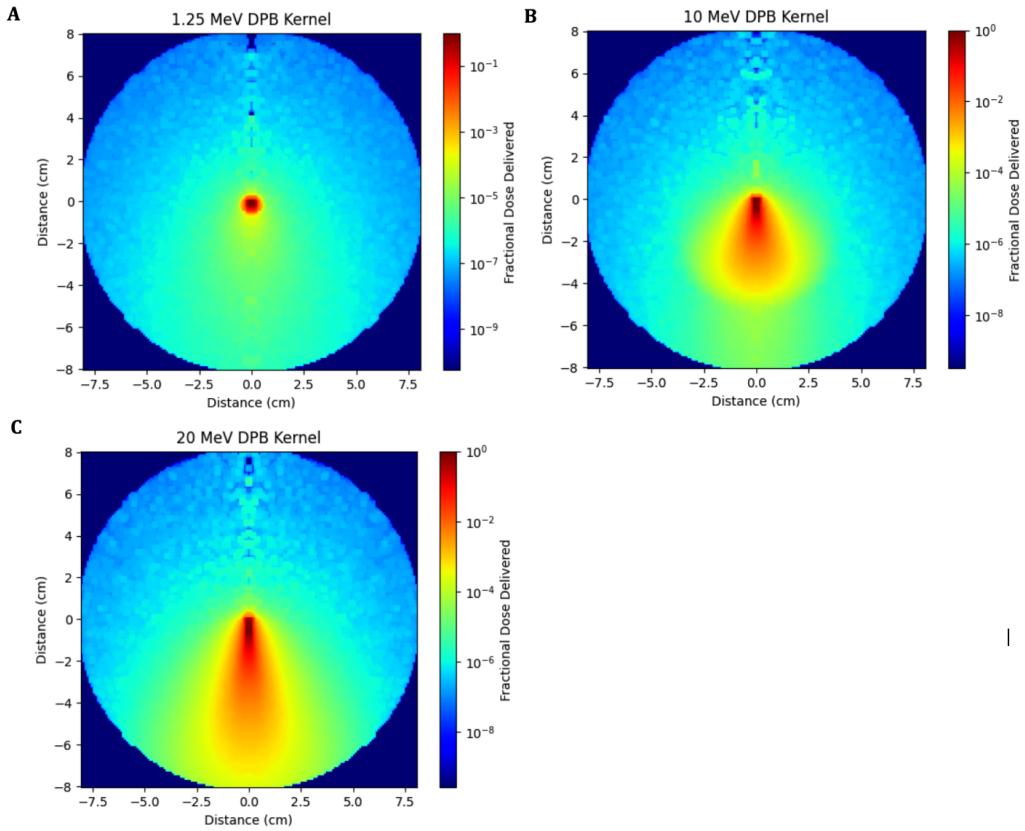

Figure 1: Display of 1.25, 10, and 20 MeV differential pencil beam (DPM) kernels in images **A**, **B**, and **C**, respectively. Intensity scale is log scaled, with distance scaling in 2D in cm.

Deliverable 2: Primary Fluence in Absence of the Phantom – Uniform Dose Profile

The inverse square law (ISL) is applied with a uniform dose profile along the horizontal axis (Figure 2) and with the phantom mask (Figure 3) without considering attenuation, where the beam is collimated to be a width of 6 cm at isocenter (SSD = 100 cm along the centeral axis). To maintain the uniform dose profile but apply the inverse square law (ISL), we first apply ISL by decreasing the uniform fluence value for a given vertical distance travelled, and then second increase the width. The beam value according inverse distance squared with reference to SSD 100 cm:

$$\Psi(y) = ISL(\mathrm{y}) = \left(\frac{\mathrm{SSD}}{\mathrm{SPD(y)}}\right)^2 \qquad \text{(line 92)}$$

The beam width for a given y value is calculated via similar triangles, where the beam width at SSD 100 cm is 6cm:

$$\tan\theta = \frac{6 \text{ cm}}{100 \text{ cm}} = \frac{w}{\mathrm{SPD\ cm}}$$

$$w(y) = \frac{6(\mathrm{SPD}(y))}{100} \text{ cm} \qquad \text{(line 98)}$$

By definition of the ISL factor above, the fluence is defined at 1 at the surface along along the central vertical axis. Since we find relative doses for a uniform phantom tissue, within the document and plots, the meanings of fluence and dose are used interchangeably, since dose and fluence only change via a mass-attenuation coefficient which is constant for a given energy and spatial location.

Deliverable 3: Attenuation in Tissue – Uniform Dose Profile

Where t is the ray-line distance through the patient, and μ is the energy dependent linear attenuation coefficient through the patient:

$$\Psi_{attenuated} = \Psi(y) \times e^{-\mu(E)\times t(x,y)} \qquad \text{(line 124)}$$

The path through the patient, t, is calculated for every point P inside the patient by finding the distance from point P to the surface of the patient vertically above it.(line 403). This method treats ray beams traveling vertically to maintain the "uniformness" of fluence in absence of the patient, as opposed to a more realistic situation where beams diverge radially, and the distance is taken to be the divergent ray path throughout the patient. The relative fluence in these two methods at the most drastic case (lowest vertical point, edge of beam) was found to be 0.409 vs 0.411 relative dose, or a 0.49% difference in the worst case.

The plotted attenuation through the patient (Figure 4) of lowest energy, 1.25 MeV, shows much more attenuation throughout the patient tissue than the 10 and 20 MeV cases. This is consistent with the expected as lower energy photons are less penetrating then higher energy (i.e. will interact less), and will lose energy faster.

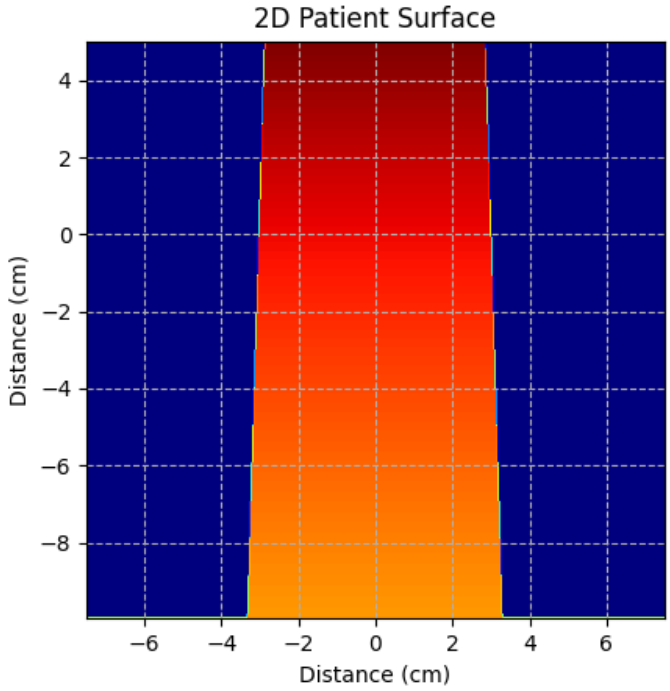

Figure 2: Fluence of beam through both air and phantom, without considering attenuation. Describes the application of ISL, in absence of the patient.

Deliverable 4

The final dose distribution is calculated at each point P(x,y) by integrating across all other points within the patient the incident fluence times appropriate differential pencil beam (DPB) value. The dose outside the patient is 0, and so post convolution these points are manually set to 0. The manual convolution is completed in polar coordinates by integrating only in a nearby area of each point P, instead of all pixels in the patient. Instead of converting from polar to cartesian at every integrand, the DPB kernels for each energy are converted to a single python dictionary (hash map) that returns only the resolution-relevant DPB kernel values for given r and theta values. The effect of the resolution of polar integration is shown visually in Figure 5 by plotting the precomputed map mentioned for a variety of resolutions.

Since the result is relative dose distribution, the mass attenuation factor within the integral is omitted (will be the same for a given energy). The differential area dA which includes the radial distance, r is directly accounted for. While $d\theta$ and dr are independent of P(x,y) and will be absorbed into the relative factor, the value r will not be.

$$D(x,y) = \int_0^{r_{max}} \int_0^{360^o} \Psi_{att}(x,y,E) \times \text{DPB}(r, \theta - 180^o) r dr d\theta \qquad \text{(line 176)}$$

The final result in Figure 6 shows the blurred edges due to scatter, and most notably the increase in anterior edge compared to either lateral edge. This can be explained due to both

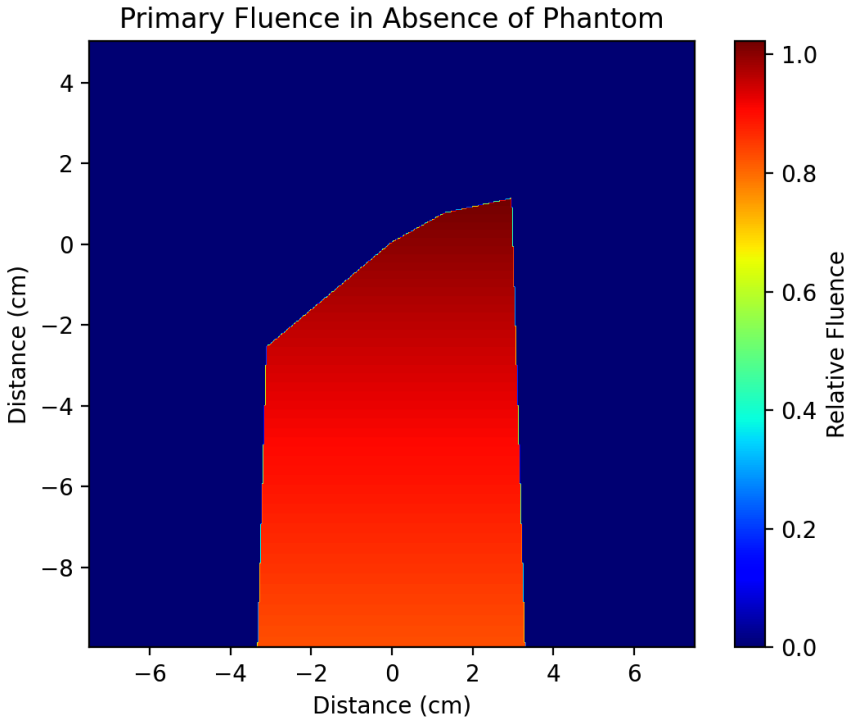

Figure 3: Display of 2D, energy independent relative fluence map in patient tissue, without including any attenuation (i.e. in absence of phantom).

the forward nature of scatter visible in the DPB kernels, as well as the increase in scatter with increasing energy. This effect creates a strong build up region as points deeper inside the patient will have the strong forward scatter coming from points anterior to (i.e. behind) it. The plots shown are computed with a resolution of dr =0.1cm, $d\theta$ = 10 Degrees, and r_{max} =8 cm for all three energies.

Deliverable 5: Comparison of Depth Dose Profiles

For each beam the attenuation and scatter both depend on energy. At higher energies we expect less attenuation per distance traveled, and more dose deposited through scatter (as described by the DPB kernels). This means at lower energies we expect sharper penumbras (less scatter effect), with a higher proportion of the beam's energy to be deposited at shallower depths. Around the edges of the beam, we expect less dose due to decreased incident scatter (for example, at a point in the center of the phantom it receives scatter from all directions, whereas on the edge only scatter from inward is received).

From the percent depth dose profiles of all three energies (Figure 7) we notice first the depth of maximum dose, d_{max}, second, the fall of dose as the beam propagates through the tissue, and third, the size of build up region:

1. **Maximum-dose depth:** As energy increases, so does the depth at which maximum dose is delivered, d_{max}. This is consistent with higher energy beams depositing the

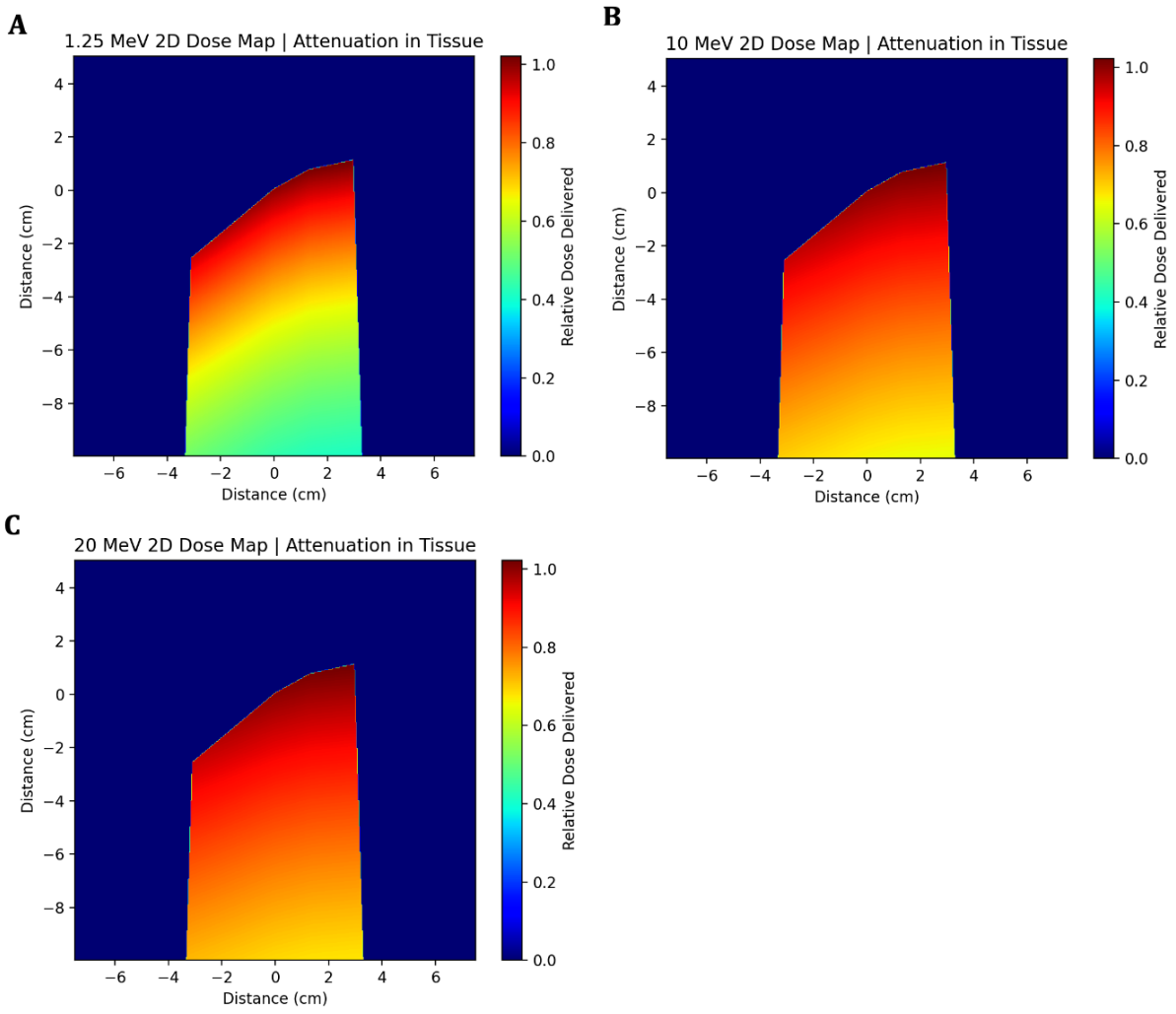

Figure 4: Display attenuation through tissue along ray paths of beam energies 1.25, 10, and 20 MeV shown in images **A**, **B**, and **C**, respectively.

bulk of the energy deeper into mediums.

2. **Dose fall off:** The 1.25 MeV beam has a much sharper fall of in dose than the 10 and 20 MeV beams, again consistent with lower energies having higher attenuation, and thus depositing more of the energy per distance.

3. **Buildup region:** The buildup region increases with energy of the beam. This is expected, and solely due to the scattering of the beam, causing lower dose near the edges of the profile. This is especially present in the edge along the central axis, due to the forward propagating nature of scatter as described visually in the DPB kernels.

Also note at the end of depth, d = 10 cm, there is a small drop off region. This region represents a drop in relative dose due to higher scatter towards the center. This drop off is expected around all edges of the 2D dose profile.

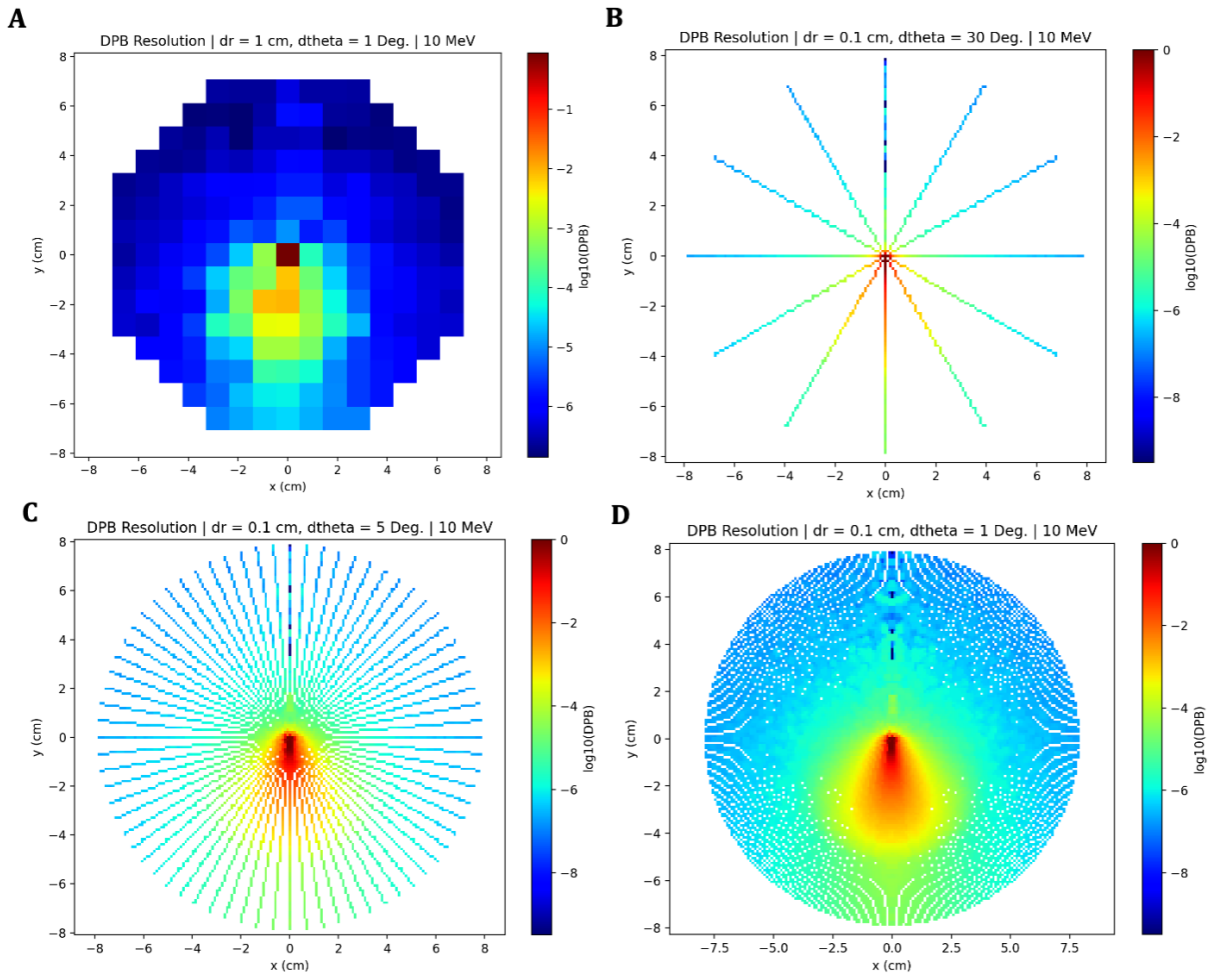

Figure 5: Display of polar resolution for varying radial and angular resolutions, used in the convolution process.

Deliverable 6: Comparison of Lateral Dose Profiles

The lateral dose profile normalized to the central axis of the patient per energy, at a depth of 4 cm (Figure 8). We notice two things:

1. **Penumbras:** The 1.25 MeV beam shows slightly sharper penumbras than the 10 and 20 MeV beams, which show no apparent difference. This can be explained by the energy dependent DPB kernels, where the 10 and 20 MeV kernels show significantly more scatter, and hence we expect the edges to be blurrier(i.e. edges have a higher effect on dose).

2. **Uneven horns:** While the 10 and 20 MeV beams have closer to flat lateral profiles, the 1.25 MeV has close to a 20% variation along the beam width. Comparing the lateral dose profile to the attenuation map, we see the same higher variation in dose with the 1.25 MeV beam, and much less variation in the 10 and 20 MeV beams. These horns

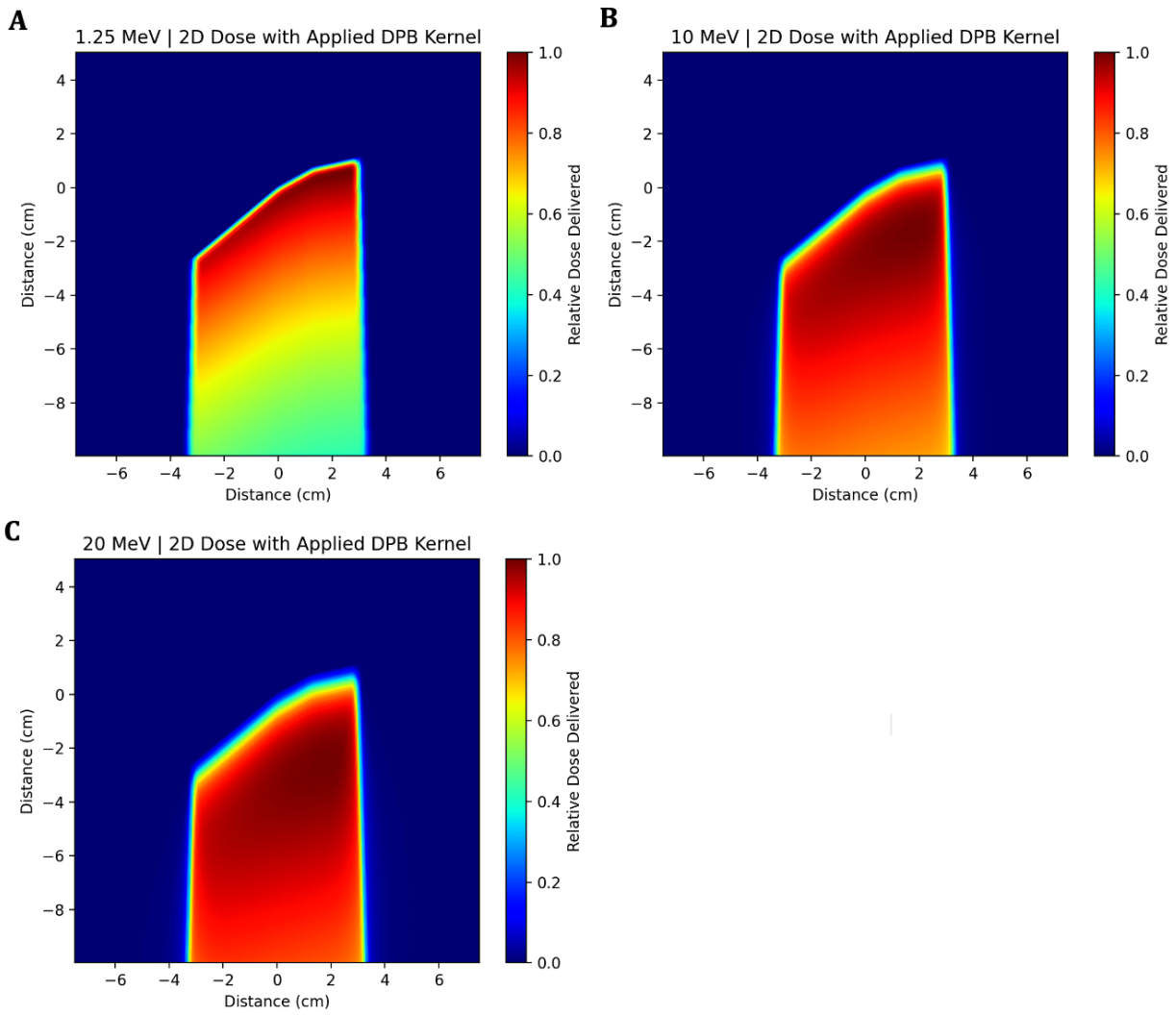

Figure 6: 2D dose distribution of 1.25, 10, and 20 MeV beam energies in images **A**, **B**, and **C**, respectively. The resolution used in all 3 images are dr =0.1cm, $d\theta$ = 10 Degrees, and r_{max} =8 cm.

can then be explained via the difference in attenuation between the different energies along with the uneven patient surface. This creates notable differences in path lengths travelled at depth = 4 cm, which are emphasized by the increase in attenuation in lower energies.

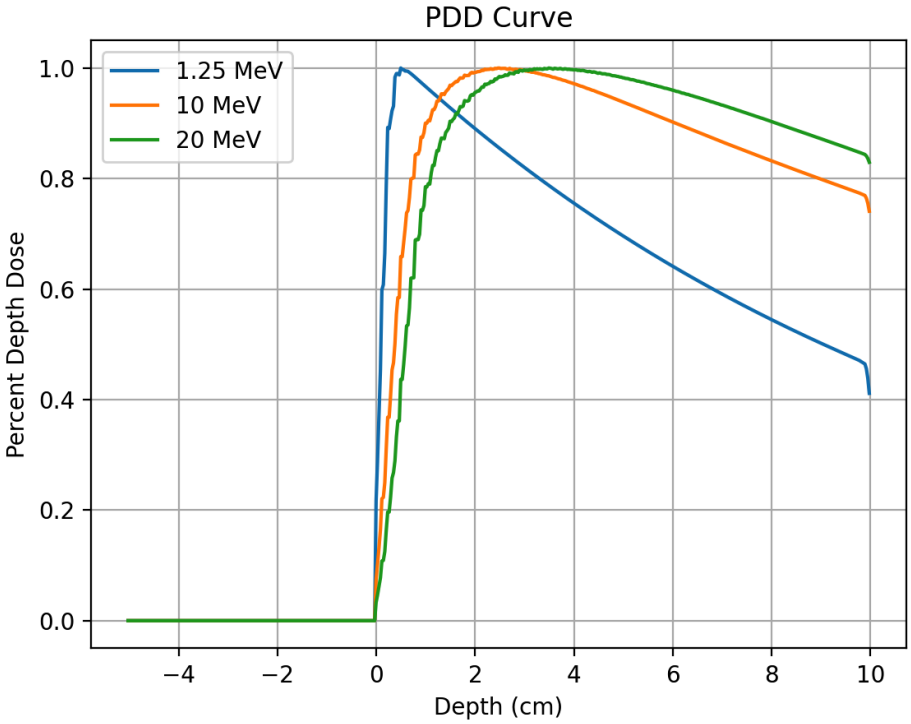

Figure 7: Percent depth dose profile of energies 1.25, 10, and 20 MeV along the central axis.

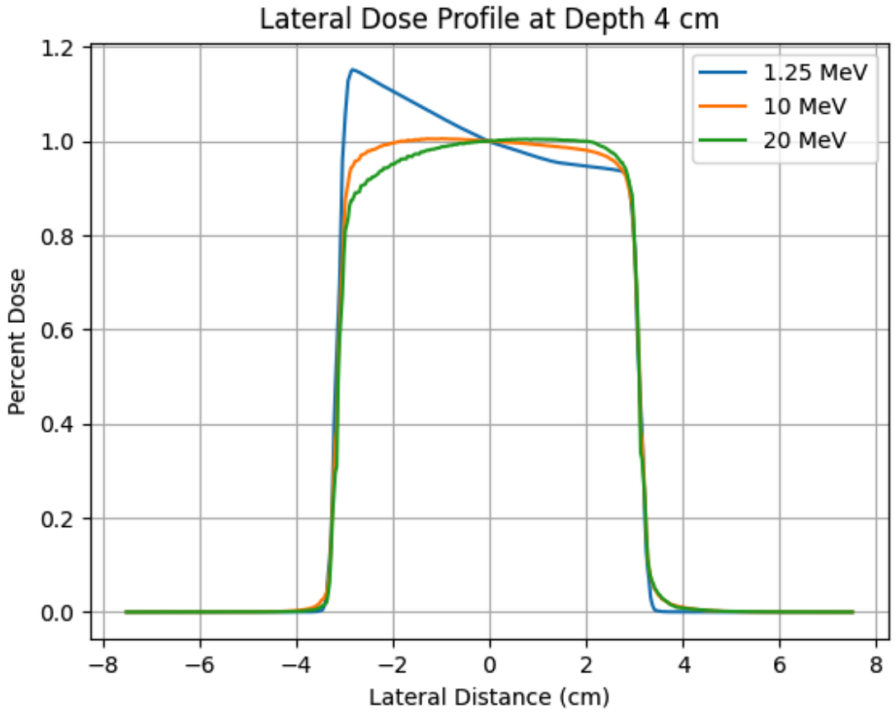

Figure 8: Lateral percent dose profile of energies 1.25, 10, and 20 MeV at a depth of 4 cm.

Discussion

1. **If the beam was poly-energetic:** The core integral would have to be across not only space, but across the energy spectrum of the beam. Within the integral, we have three energy dependencies:

   (a) The attenuation through tissue and hence fluence at any point P is energy dependent. A differential energy fluence will be used describing the energy spectrum of the beam.

   (b) The scatter is energy dependent (i.e. DPB(E)). A spectrum of DPB kernels would have to be used, or a small set of DPB kernels to be interpolated from.

   (c) The mass-attenuation coefficient is no longer spatially independent since it is a function of energy (i.e. the process is no longer shift-invariant), and now needs correction within the integral. This value may be linearly interpolated from a table, possibly referenced to the NIST data base.

   Where $\Psi'(r, \theta, E)$ represents the differential energy fluence at some point r, θ, and energy from some point P(x,y) including the effects of attenuation and ISL, the dose at some point P will now be calculated in the code as:

$$D(x,y) = \int_0^{r_{max}} \int_0^{360^o} \int_E \left(\frac{\mu}{\rho}\right)_E \Psi'_{att}(x,y,E) \times \text{DPB}(r, \theta - 180^o, E) r dr d\theta dE$$

2. **Assumptions on beam divergence with respect to kernels:** The DPB kernels describe how a single deposition of **forward propagating** fluence scatters its energy in the surrounding medium. In Figure 1, the beam propagates from anterior to posterior (or top to bottom looking at the graph). It is assumed in the computation that the photons are traveling perfectly parallel to the vertical axis. This is not strictly true, as photons diverge from the point source radially. In the computation, this radial divergence is ignored when applying the DPB kernels. To account for this, the DPB kernels need to be rotated appropriately as a function of P' (i.e. r and θ). This can be accomplished via scipy's rotate function: `rotate(arr, theta, reshape=False)` where $\theta = \arctan(\Delta x / SPD)$, and Δx is the horizontal distance from the central axis.

3. **Other assumptions:** More realistic situations may require factors such as beam hardening due to the filter used (such as flattening filter) which cause depth dependent dose profile horns, or non-linear system dependence, such as photon-photon interactions at higher energies. Such non-linear corrections would create the convolution method invalid, which requires linear superposition.